

## Highlights

### **Reducing RES Droughts through the integration of wind and [solar](#) PV**

Boris Morin, Aina Maimó Far, Damian Flynn, Conor Sweeney

- RES droughts are analysed using 45 years of hourly wind and [solar](#) PV generation data
- RES droughts from C3S-Energy and ERA5-Atlite datasets are compared
- Adding [solar](#) PV to a wind-dominated system reduces RES drought frequency and duration
- Validated RES datasets are crucial to accurately identify RES drought extremes

# Reducing RES Droughts through the integration of wind and solar PV

Boris Morin<sup>a,\*</sup>, Aina Maimó Far<sup>a</sup>, Damian Flynn<sup>b</sup>, Conor Sweeney<sup>a</sup>

*<sup>a</sup>School of Mathematics and Statistics, University College Dublin, Belfield, Dublin  
4, Dublin, D04 V1W8, Ireland*

*<sup>b</sup>School of Electrical and Electronic Engineering, University College Dublin, Belfield,  
Dublin 4, Dublin, D04 V1W8, Ireland*

---

\*Corresponding author

*Email addresses:* `boris.morin@ucdconnect.ie` (Boris Morin ),  
`aina.maimofar@ucd.ie` (Aina Maimó Far), `damian.flynn@ucd.ie` (Damian Flynn),  
`conor.sweeney@ucd.ie` (Conor Sweeney)

---

## Abstract

Increasing the share of electricity produced from renewable energy sources (RES), combined with RES dependence on weather, poses a critical challenge for energy systems. This study investigates the importance of the balance between wind and [solar](#) photovoltaic (PV) capacity on periods of low renewable generation, known as RES droughts. Three different RES [models](#) [datasets](#) are used to estimate the capacity factors for different scenarios of installed capacities for wind and [solar](#) PV power. The skill of the RES [models](#) [datasets](#) is quantified by comparing capacity factor time series to observed hourly data and by assessing their representation of observed RES droughts. The RES [models](#) [datasets](#) are used to generate a 45-year hourly time series of RES capacity factor, enabling analysis of the frequency, duration and return periods of RES droughts at a climatological scale. Results show the importance of using an accurate, validated RES [model-dataset](#) for RES drought risk assessment. The addition of [solar](#) PV capacity to a wind-dominated system results in a significant reduction in the frequency and duration of RES droughts, while also reducing extremes and seasonal [RES](#) drought patterns. These findings underscore the importance of diversification in RES capacity to enhance energy security and resilience.

*Keywords:* RES Drought, Wind Power, Solar PV Power, Renewable Energy Sources, Return Periods

---

## 1. Introduction

2     The EU aims to generate at least 69% of its electricity from renewable  
3     energy sources (RES) by 2030, up from 41% in 2022 [1]. While this transition  
4     is essential for reducing greenhouse gas emissions, it also highlights the chal-  
5     lenge of managing the variability of weather-dependent energy sources such  
6     as wind and [solar](#) photovoltaic (PV) power. This challenge is [compounded](#)  
7     [amplified](#) by the increasing electrification of energy sectors, which places  
8     greater demand on the power system and makes it more sensitive to mete-  
9     orological conditions [\[2, 3, 4\]](#), [both in historical \[2\] and future climates \[3\]](#).  
10    Periods of low renewable generation, known as *Dunkelflaute* or RES droughts,  
11    pose significant risks to system adequacy and energy security, emphasising  
12    the need for a resilient energy system to meet both growing electricity de-  
13    mand and decarbonisation targets.

This study focuses on Ireland, a region with a strong reliance on wind power, which has ambitious targets for PV power expansion. This case study provides valuable insights into the potential benefits of diversifying the renewable energy mix on RES droughts. The performance of different RES models are compared, and a 45-year time series of RES generation is produced. The results highlight the role of increased PV capacity in reducing RES drought risks, offering insights for policymakers and energy planners.

For this study, RES drought events do not have a fixed definition, with various approaches present in the literature. One common method defines a RES drought event as occurring when as a period during which the average capacity factor (CF) remains below a fixed threshold for a given duration, following the methodology used in other research [5, 6, 7, 8]. Alternative methods exist for defining specified duration. For example, Kaspar et al. [5] used this method to investigate the shortfall risks of low wind and solar PV generation in Europe, with a focus on Germany, testing multiple CF thresholds and durations. Similarly, Mockert et al. [7] examined the link between weather regimes and RES droughts in Germany using a 48-hour rolling window under a threshold to define RES droughts. One approach uses relative CF thresholds that change. Similar fixed-threshold approaches have also been applied using CF series reconstructed through machine learning in regions such as Japan [6] and Hungary [8].

Alternative methods adjust the CF threshold dynamically over the year to account for seasonal variations in renewable energy generation [9, 10, 11, 12, 13]. Another common method relies on percentile-based thresholds, where drought events are defined by identifying production. Raynaud et al. [9] defined RES droughts as sequences of days with renewable electricity generation below a threshold that varies seasonally, a methodology later adapted for India [11]. Building on this, Kapica et al. [13] compared the likelihood of increased RES droughts in Europe under different climate models. Other studies have defined RES droughts based on deviations from daily mean production: Rinaldi et al. [10] applied these in the U.S. Western Interconnection to quantify the benefits of long-term storage, while Brown et al. [14] examined weekly timescales to explore meteorological influences on the most severe RES drought events. Another method defines RES drought indices based on metrics commonly used in hydro-meteorology to characterise RES droughts [12]. This approach identifies periods of unusually low generation relative to historical production levels, typically based on using the lowest production percentiles [12, 15]. Additionally, some studies combine these definitions with

metrics that incorporate the demand side of energy consumption, analysing the balance between supply and demand during drought periods [9, 10, 12, 15]. Bracken et al. [15] used this approach to analyse RES droughts at different time scales in the U.S. [15], and Lei et al. [16] used it to quantify RES droughts in wind-PV-hydro systems in China.

In addition to examining periods of low renewable electricity generation, several studies also explore the periods when the imbalance between renewable generation and electricity demand (residual demand) is high. Raynaud et al. [9] showed the difference between RES droughts and high residual demand events in a hypothetical fully renewable system composed of wind, solar PV and run-of-the-river hydropower. Similarly, Allen and Otero [12] also defined a standardised index based on meteorological droughts to address residual demand, whose correlation to the electricity generation index is mostly negative (as expected, although quite low anticorrelations and even small positive correlations appear for some European countries). This index was also applied to the U.S. by Bracken et al. [15], revealing a consistent increase in the RES drought magnitude when demand is considered, despite showing differing results across regions.

In this paper, the focus is exclusively on ~~energy generation, and a renewable electricity generation, to keep the focus on RES droughts driven by the weather.~~ A fixed threshold approach is used to define RES droughts~~is used,~~ which facilitates consistent inter-comparison between scenarios with different installed wind and solar PV capacities. The case study used in this paper is Ireland, a region where most RES generation comes from wind power and with ambitious targets for solar PV power expansion. This provides valuable insights into the potential benefits of adding solar PV installations in wind-dominated countries.

RES droughts are identified using onshore wind and solar PV CF time series. In this study, three different datasets are used ~~and compared,~~ all of which are driven by the ERA5 ~~data~~~~reanalysis~~ [17]. Two of the datasets are part of C3S Energy (~~C3S-E~~C3SE), an energy-based operational dataset produced by the EU Copernicus Climate Change Service ~~[18, 19]~~[18]. One of the ~~C3S-E~~C3SE datasets provides CF time series aggregated at the national scale, while the other provides the CF time series at each grid point, at the ERA5 resolution of 0.25°. The third dataset ~~produced by the authors~~ was generated using the Atlite model [20], which converts the ERA5 atmospheric data to a generation time series using specified wind turbine and PV panel models. Atlite is an open-source tool developed by PyPSA [20] and ~~is widely~~

has been used for estimating wind and ~~PV-generation~~ [7, 21, 22, 23] solar PV generation in order to study RES droughts in Germany [7].

Generic datasets for wind and solar PV CF are often used for the quantification of RES droughts. Despite undergoing a general validation process, they are often not fully representative of each geographical location, and can show differences in the number of RES drought events subsequently identified [24]. This study evaluates the skill of a dataset developed for the European region (C3SE) when applied to a specific country; Ireland. In particular, the analysis explores the impact of using a generic versus a tailored dataset on RES drought assessments, in the context of a transition from a wind-dominated system to one with a greater share of solar PV capacity.

The aim of this study is to answer two questions which are relevant for systems with a large share of RES generation:

- Do generic datasets have sufficient skill to reliably quantify RES drought events for specific countries?
- How does the integration of solar PV capacity into a predominantly wind-based system alter the characteristics of RES drought events?

The datasets used in this study are detailed in section ??2, which describes their characteristics and relevance for evaluating RES droughts. Section ??3 outlines the RES ~~models-datasets~~ used to simulate wind and solar PV generation and provides the methodology for defining and identifying RES drought events, including the thresholds and metrics applied. In section ??, ~~the models~~ 4, the datasets are first verified against observed energy data to assess their accuracy, followed by an analysis of RES drought occurrences for two scenarios with different ratios of installed wind to solar PV capacities. Finally, section ??5 offers a discussion of the results in the context of energy reliability and future planning, followed by the main conclusions and recommendations for further research.

## 2. Data

This study uses publicly available datasets to construct and validate the ~~models-datasets~~ for estimating the CF of wind and ~~PV-energy~~ solar PV power. The primary data sources include: EirGrid and SONI, the transmission system operators (TSO) for the Republic of Ireland and Northern Ireland, respectively; the ERA5 reanalysis dataset; and the ~~C3S-E-datasets~~ C3SE dataset.

## 125 2.1. Wind and solar PV Capacity and Availability

126 EirGrid, the TSO for the Republic of Ireland, and SONI, the Northern  
127 Ireland TSO, provide detailed datasets on all wind and solar PV farms across  
128 the island of Ireland (Republic of Ireland and Northern Ireland) from 1990  
129 to the present [25]. These datasets include information such as each farm’s  
130 installed capacity, name, and connection date. To enhance the accuracy of  
131 this data, the longitude and latitude for each farm were manually determined  
132 through online searches. For simplicity, this data will be referred to as orig-  
133 inating from EirGrid, as all-island data was directly obtained from EirGrid,  
134 and the combined regions of the Republic of Ireland and Northern Ireland  
135 will be referred to as Ireland throughout the remainder of this document.

136 The spreadsheet available from the EirGrid website contains two key vari-  
137 ables: generation and availability. Generation and availability values are  
138 available from 2014 onward for wind power and from 2018 onward for solar  
139 PV power, although solar PV availability data only became present in the  
140 Republic of Ireland in 2023. Generation is the energy that a RES farm  
141 actually contributed to the grid, which may include limitations introduced  
142 by the TSO to maintain grid stability, such as constraints and curtailment.  
143 Availability represents the energy that would have been generated from a  
144 RES farm if no grid constraints had been applied, making it representa-  
145 tive of the weather-related response. ~~Generation and availability values are~~  
146 ~~available from 2014 onward for wind power and from 2018 onward for PV~~  
147 ~~power, although PV availability data only became present in the Republic of~~  
148 ~~Ireland in 2023.~~ This study focuses on availability for all analyses.

## 149 2.2. Atmospheric Variables

150 ~~Atlite and C3S-E datasets~~ All of the datasets used in this study are driven  
151 by data from the ERA5 reanalysis [17], produced by the European Centre for  
152 Medium-Range Weather Forecasts (ECMWF). This global gridded dataset  
153 provides hourly atmospheric variables from 1940 to the present at a hor-  
154 izontal resolution of 0.25°. ~~It is widely used for estimating PV and wind~~  
155 ~~energy [7, 18, 14, 26].~~ Table 1 lists the relevant ERA5 variables ~~used by Atlite~~  
156 ~~and C3S-Energy.~~

## 157 2.3. C3S Energy

158 The EU Copernicus Climate Change Service developed the ~~C3S-E~~ C3S-Energy  
159 (C3SE) renewable energy dataset for Europe [18], using ERA5 atmospheric  
160 variables and weather-to-energy models. This dataset provides hourly CF

Table 1: ERA5 variables used to calculate wind and solar PV generation

ERA5 name	variable
100 metre zonal and meridional wind speed	$u_{100}, v_{100}$
2 metre temperature	$t2m$
Surface net solar radiation	$ssr$
Surface solar radiation downwards	$ssrd$
Top of atmosphere incident radiation	$tisr$
Total sky direct solar radiation at surface	$fdir$

for wind and ~~PV energy~~ solar PV power from 1979 to the present. The data are available on the same grid as the ERA5 data, which has a horizontal resolution of  $0.25^\circ$ . The time series are also available for download at two aggregated scales: regional (NUTS 2) and national.

The ~~C3S-E dataset estimates wind energy~~ wind CF in C3SE was calculated using wind speeds at 100 metres ( $u_{100}, v_{100}$ ) and a standard turbine model, the Vestas V136/3450, with a fixed hub height of 100 meters. ~~This choice is based on expert advice and the trend in wind turbine installation. The PV generation model used by C3S-E uses two~~ As data on wind turbine fleet locations and specifications are difficult to obtain across Europe, C3SE assumes a homogeneous distribution of wind turbines across the ERA5 variables: grid. While this approach does not capture the precise capacity factors reported by grid operators, it provides a well-correlated time series that effectively represents the impact of climate variability on wind power generation. The C3SE solar PV CF was also calculated for the ERA5 grid. It is derived from meteorological data, including surface solar radiation downwards ( $ssrd$ ) and air temperature ( $t2m$ ). ~~PV generation is calculated multiple times, using the same model with different azimuth and tilt angles. The results are aggregated based on a statistical distribution of the module angles based on the geographical, using a reference solar PV plant model. This model incorporates empirical calculations for key system components such as optical losses, module efficiency, and inverters. The final CF accounts for a mix of module orientations typical for each~~ location [27].

### 3. Methods

This study ~~uses three datasets to analyse RES droughts across the island of Ireland. Data downloaded from C3S-E were used to obtain two datasets:~~



analyses RES droughts using onshore wind and solar PV CF time series from three datasets: two from C3SE; one based on national-level data (C3S-E-N), and another C3S NAT) and the other on grid-level data (C3S-E-G). The third dataset was computed C3S GRD), and a third dataset derived using the Atlite model (AtliteATL).

### 3.1. ~~C3S-Energy~~ C3S Energy National: C3S NAT

For national-level analyses, the aggregated CF time series provided by C3S-E were used at two. The C3S NAT dataset is created by combining two inputs provided by C3SE at the corresponding NUTS levels: Republic of Ireland (NUTS0: IE) and Northern Ireland (NUTS2: UKN0). These are based on the assumption by C3S-E. The two inputs are combined, using the actual installed capacity as weights. This dataset assumes that RES generation occurs at every ERA5 grid point in Ireland. We computed a weighted average of these, based on the installed capacity of each one, to represent the total CF for Ireland.

### 3.2. ~~C3S-E~~ C3S Energy Gridded: C3S GRD

The gridded dataset from C3S-E was used to create CF datasets which account for the location of RES farms in Ireland. A list C3S GRD dataset uses, as inputs, the actual locations of the RES farms in Ireland was compiled, including each farm's latitude, longitude and installed capacity. Using these coordinates, the nearest grid point on the C3S-E grid was identified for each farm. The CF values from the C3S-E dataset corresponding to these grid points were retrieved, and the CF from C3SE over the ERA5 grid. For each farm, the CF from the nearest grid point on the C3SE dataset was selected. A weighted average of the CF values was calculated, with the installed capacity of each farm serving as the weight, to construct the associated with each farm, using the farm's installed capacities, was used to produce the total CF time series for Ireland. This process resulted in a time series of RES generation for each energy source (wind and PV) for Ireland, which takes the location of the RES farms into account.

### 3.3. Atlite: ATL

Atlite transforms weather data into energy data using the gridded ERA5 data and. The ATL dataset is produced using the Atlite model. Atlite allows the user to define the wind turbine power curve and PV panel model to use when converting weather variables to wind and solar PV generation.

222 ~~The Atlite model takes as inputs the locations of existing RES farms, as~~  
 223 ~~described in C3S-E-G. RES farms and ERA5 data for weather variables: wind~~  
 224 ~~speed at 100 metres ( $u_{100}$ ,  $v_{100}$ ) are used to calculate for~~ wind generation,  
 225 ~~while the ERA5 and~~ radiation variables ( $ssr$ ,  $ssrd$ ,  $tisr$ , and  $fdir$ ) ~~and along~~  
 226 ~~with~~ air temperature ( $t2m$ ) ~~are used to calculate for solar~~ PV generation.  
 227 ~~A key distinction between C3S-E and Atlite lies in their representation of~~  
 228 ~~wind turbines and PV panels~~ The output of the Atlite model is a generation  
 229 ~~time series, which is divided by the total capacity to transform it back into~~  
 230 ~~CF. The selection of the wind turbine power curve and PV panel model~~  
 231 ~~represents the key difference between this dataset and C3S GRD. This study~~  
 232 identifies the most appropriate wind turbine power curve to use from the 121  
 233 power curves, ~~each at five different levels of smoothing,~~ made available by  
 234 Renewables.ninja [28]. ~~The selection of a specific wind turbine and PV panel~~  
 235 ~~characteristics is further discussed and explained in section 4.1, and selects~~  
 236 ~~the PV panel model out of the options available within Atlite.~~

### 237 3.4. Energy Scenarios

238 ~~The three datasets provide CF time series for both wind and solar PV.~~  
 239 In addition to analysing ~~wind and PV generation~~ the CF of wind and solar  
 240 ~~PV~~ separately, a combined CF was computed for each ~~model-dataset~~ by  
 241 averaging wind and ~~PV-generation~~ solar PV CF, weighted by their installed  
 242 capacities at the end of 2023 (5.9 GW for wind power and 0.6 GW for solar  
 243 power). This configuration is referred to as the 91W-9PV scenario, reflecting  
 244 the distribution of 91% wind and 9% solar PV capacity. Given that solar  
 245 PV capacity in Ireland is low in 2023, and to explore how a more balanced  
 246 distribution of wind and solar PV capacities might impact RES droughts, this  
 247 study also considered a second scenario, referred to as 57W-43PV, where the  
 248 installed solar PV capacity is assumed to increase to 8.6 GW, while wind  
 249 capacity rises to 11.45 GW. These values are based on targets outlined in  
 250 the roadmap published by the 2024 Climate Action Plan [29]. This study  
 251 does not include offshore wind in the analysis. Recent reports suggest that  
 252 even by 2030, Ireland is unlikely to have any significant new offshore wind  
 253 farms, with projected offshore capacity expected to remain near zero using  
 254 realistic scenarios [30].

255 New time series were generated for both the ~~Atlite and C3S-E-G PV~~  
 256 ~~models~~ ATL and C3S GRD solar PV datasets, incorporating a revised distri-  
 257 bution of installed capacity across Ireland as specified in the roadmap [31].  
 258 For wind power, the CF time series remains unchanged, as significant shifts

259 in the location of wind farms are not expected. In total, twelve CF time  
260 series were analysed in this study, six for individual wind and solar PV CF  
261 (three ~~models~~ datasets for each source) in the 91W-9PV scenario, and an  
262 additional six time series that include the combined CF for 91W-9PV and  
263 57W-43PV scenarios across the different ~~models~~ datasets.

264 It is important to note that the specific capacity values used in this study  
265 are illustrative and are not intended to reflect ~~precise~~ accurate future reali-  
266 ties. Instead, they serve to explore the impact of transitioning from a wind-  
267 dominated system (91W-9PV) to a more evenly distributed system (57W-  
268 43PV). This approach allows for a comparative analysis between the two  
269 scenarios, assessing how the balance of RES capacity affects the occurrence  
270 of RES droughts.

271 In summary, for each of the three datasets (ATL, C3S GRD and C3S  
272 NAT) four energy scenarios are examined:

- 273 • Wind Power - based on the actual capacity at the end of 2023
- 274 • Solar PV Power - based on the actual capacity at the end of 2023
- 275 • Combined RES / 91W-9PV - based on the actual capacity at the end  
276 of 2023
- 277 • Combined RES / 57W-43PV - based on the projected capacity for 2030  
278

### 279 3.5. RES Drought Definition

280 In this study, a RES drought event was defined as occurring when the  
281 24-hour moving average of CF remains below a fixed threshold of 0.1 for  
282 a period of longer than 24 hours. ~~The choice of this threshold is somewhat~~  
283 ~~arbitrary, but aligns with similar studies on low renewable energy production~~  
284 ~~[5, 6, 8].~~ By using a 24-hour moving average, fewer but longer-lasting events  
285 were captured compared to using the raw CF time series, which can be more  
286 sensitive to short-term fluctuations. The 24-hour rolling average also avoids  
287 potential masking of day-long events due to their start time. A fixed thresh-  
288 old approach was chosen in this study to enable consistent inter-comparison  
289 between datasets.

290 The moving average approach smooths out short-term fluctuations, so  
291 that brief periods above the threshold do not interrupt an otherwise continu-  
292 ous low-CF period (Fig. 1). This means that a single hour above the threshold

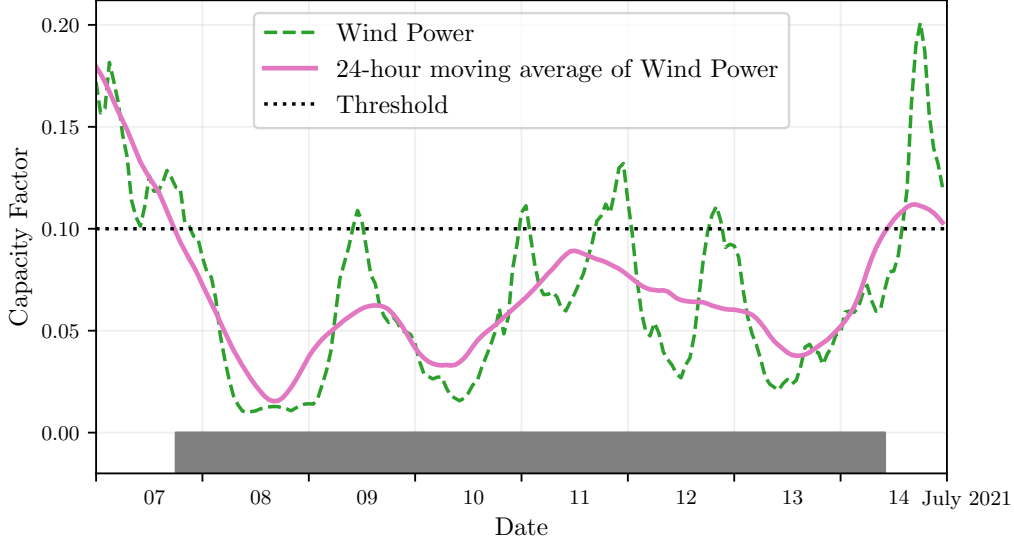


Figure 1: Wind time series of CF (green) and its 24-hour moving average (pink) from the 7th to the 15th of July 2021. The black dashed line indicates the CF threshold. The grey bar shows the period identified as a wind drought under our definition

293 does not "break" a [RES](#) drought event if it is surrounded by prolonged low-  
 294 generation hours. As a result, fewer but longer-lasting [RES](#) drought events  
 295 are identified, which may better reflect ~~real-world~~ [actual](#) conditions where  
 296 energy supply constraints persist over extended periods.

## 297 4. Results

### 298 4.1. Verification

299 The accuracy of the datasets used in this study was verified, before con-  
 300 tinuing to the analysis of RES droughts. For the verification process, time-  
 301 varying values of installed capacity were used to account for changes in RES  
 302 development over the verification period. This step allowed us to assess how  
 303 well the datasets represent the production of renewable energy by compar-  
 304 ing them against observed data. [This validation step evaluates how well the](#)  
 305 [datasets represent actual renewable energy production by comparing them](#)  
 306 [against observed data. The overall statistical distribution of CF values for](#)  
 307 [wind \(2014–2023\) and solar PV \(2023\) is presented in the violin plots in](#)  
 308 [Fig. 2. These plots illustrate the density of CF values for each dataset.](#)

309 highlighting their differences and alignment with observations. The results  
 310 indicate that ATL aligns more closely with OBS for wind, while all datasets  
 311 exhibit similar distributions for solar PV.

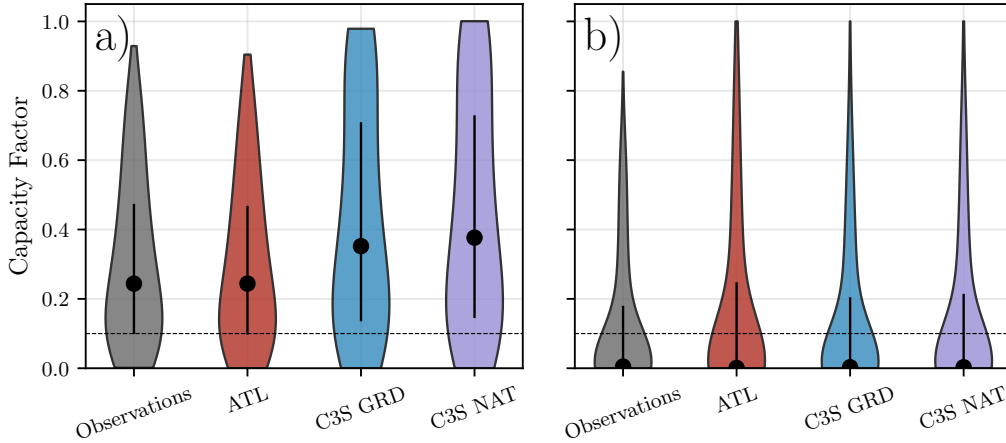


Figure 2: Violin plots of CF distributions for a) wind and b) solar PV for the Observations (grey) and the three datasets: ATL (red), C3S GRD (blue), and C3S NAT (purple). The black dot shows the median values, while the black vertical lines represent the first and third quartiles. The black dashed line indicates the threshold of 0.1 used in the study to identify RES droughts

#### 312 4.1.1. Wind Energy

313 The ~~C3S-E~~ C3S datasets use the Vestas V136/3450 wind turbine power  
 314 curve ~~Fig. 3a~~ (Fig. 3a). The Atlite model allows the user to specify the power  
 315 curve. We considered the 121 power curves available for download from  
 316 Renewables.ninja [28]. For each power curve, Renewables.ninja also provides  
 317 four associated smoothed power curves. The smoothing is done using a Gaus-  
 318 sian filter with different standard deviations that depend on the wind speed.  
 319 A separate wind CF time series for Ireland was generated for each of the  
 320 wind turbine power curves and smoothing levels.

321 The performance of each CF time series is then assessed based on four skill  
 322 scores: correlation coefficient (CC), root mean square error (RMSE), mean  
 323 bias error (MBE), and the percentage of overlap. The percentage of overlap  
 324 quantifies the similarity between the observed and modelled distributions. It  
 325 is a positively oriented skill score, where 100% shows full agreement between  
 326 the two distributions, and 0% indicates no overlap. The histograms of hourly

CF values for the most recent decade (2014-2023) are used to calculate this skill score.

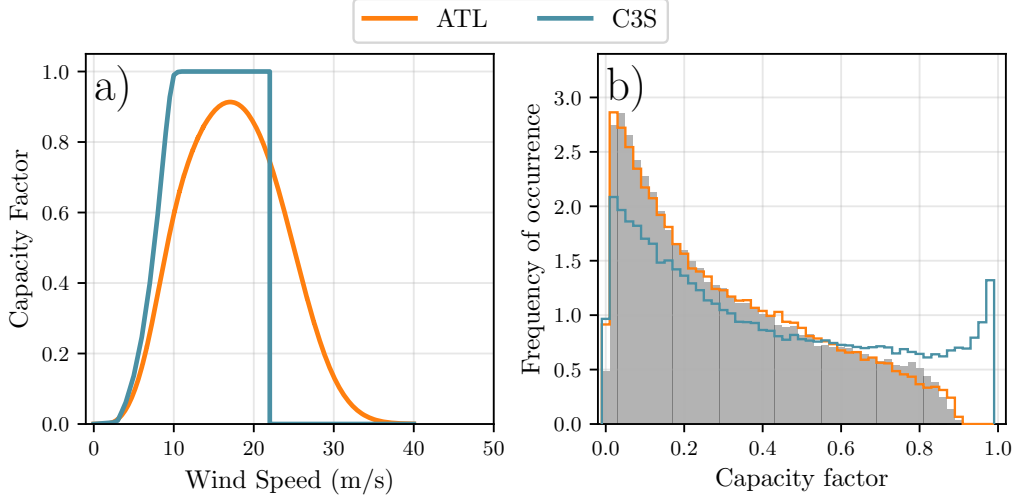


Figure 3: a) Power curves of the Enercon E112.4500 with a  $0.3w$  smoothing filter used by ~~Atlite~~-the ATL dataset (orange) and the Vestas V136/3450 used by ~~C3S-E~~-the two C3S datasets (blue) b) Histograms of wind CF for Ireland ~~from Atlite~~-for the ATL dataset (orange), ~~C3S-E~~-the C3S datasets (blue) and Observed (shaded)

Based on these metrics, the most representative power curve for Ireland is the Enercon E112.4500 power curve with the  $0.3w$  smoothing filter. The smoothing of the wind turbine power curve represents losses associated with each turbine, as well as losses such as wake effects between turbines, which are important when modelling wind energy on larger spatial scales. The histogram in Fig. 3b shows that the ~~C3S-E~~-~~C3SE~~ power curve tends to underestimate low CF values and overestimate higher ones, whereas the smoothed ~~Atlite~~-ATL power curve more closely follows the observed wind availability data. This is further supported by the percentage of overlap which is higher for ~~Atlite~~-ATL (97.2%) than for ~~C3S-E~~-~~C3SE~~ (83.2%), indicating better agreement with observed data.

The effect of the difference between the power curves is also visible in Fig. 4, which shows a density plot of wind CF values. The two ~~C3S-E~~-~~C3S~~ datasets are shown to overestimate the observed CF, whereas the ~~Atlite~~-ATL dataset is in good agreement with the observed data. The skill scores presented in Table 2 show that ~~Atlite~~-ATL performs better than the

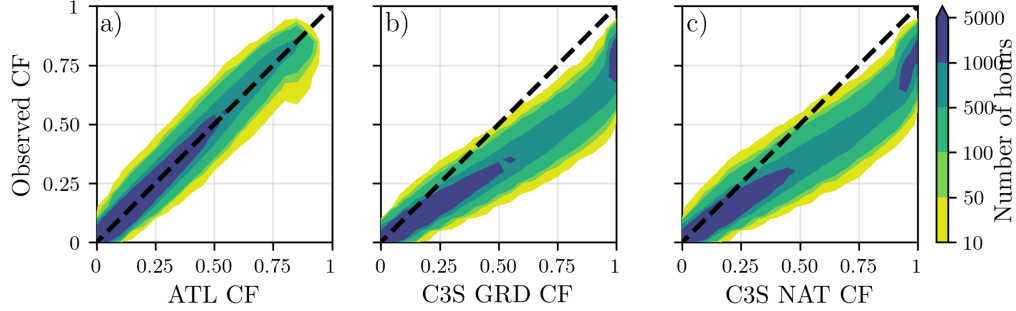


Figure 4: Wind CF density plot of the observed CF (vertical axes) and modelled (horizontal axes) CF data for the a) ~~Atlite~~ATL, b) ~~C3S-E-G~~C3S GRD and c) ~~C3S-E-N~~C3S NAT datasets

345 ~~C3S-E~~ two C3S datasets for all of the skill scores.

	<del>Atlite</del> ATL	<del>C3S-E-G</del> C3S GRD	<del>C3S-E-N</del> C3S NAT
CC	0.981	0.972	0.970
RMSE	0.045	0.177	0.162
MBE	-0.003	0.137	0.121

Table 2: Skill scores for wind power for the three datasets compared to observed data

346 Fig. 5 shows the average annual number of wind drought events during the  
 347 2014 to 2023 validation period. The figure reveals that ~~Atlite~~ATL presents  
 348 the best overall agreement with the observed frequency and duration of wind  
 349 drought events. This pattern is particularly evident for shorter-duration  
 350 events, which are the most frequent.

351 This verification for wind generation data highlights the importance of  
 352 selecting a representative wind turbine power curve for the region being  
 353 analysed. The ATL dataset, which uses a representative wind turbine power  
 354 curve, is skilled at reproducing wind CF and RES droughts over Ireland. On  
 355 the other hand, the power curve used for both C3S GRD and C3S NAT  
 356 is not representative for Ireland, as it severely overestimates generation,  
 357 underestimating the occurrence of RES droughts. This highlights a problem  
 358 with using generalised datasets for analysing RES droughts: biases severely  
 359 affect their ability to accurately reproduce RES drought events. The skill  
 360 scores for the three datasets (Tab. 2) show only a small difference in their  
 361 ability to reproduce the changes in CF, as seen by their similar CC scores.

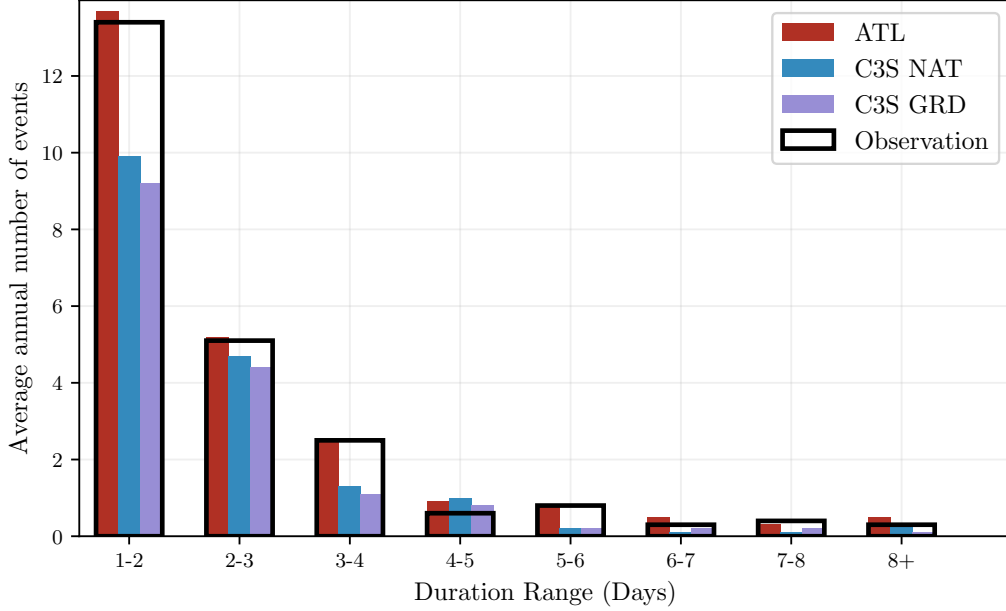


Figure 5: Average annual number of wind drought events for ~~Atlite~~-ATL (red), ~~C3S-E~~ ~~G~~-C3S GRD (blue), ~~C3S-E-N~~-C3S NAT (purple), and the observed data (black outline). The wind droughts are identified from 2014 to 2023, considering the actual capacity of the system at any given time

However, their ability to reproduce the actual CF values is much lower than that of ATL, with RMSE scores almost four times bigger for the two C3S datasets. There is a clear bias towards an overestimation of CF, seen in the MBE values, which leads to the underestimation of RES droughts. This highlights the need to use regionally verified datasets to assess RES droughts.

#### 4.1.2. *Solar* PV Energy

The Atlite model allows the user to select certain PV panel characteristics. In this study, the three PV panel types available in the Atlite model were considered (CSi, CdTe, Kaneka). Following the same methodology as in the previous section, the three available models were compared using four skill scores (CC, RMSE, MBE, and the percentage of overlap). Based on the best-performing metrics, the ~~Breyer~~-Beyer PV panel model was selected [32], using the Kaneka Hybrid panel option. For all *solar* PV farm locations, the azimuth angle is fixed at 180°(due south), and the optimal tilt angle option



377 is applied.

378 The solar PV installed capacity available on the spreadsheets from Eir-  
 379 Grid represents the Maximum Export Capacity (MEC) and does not ac-  
 380 curately reflect the installed solar PV capacity. To enable actual solar PV  
 381 generation potential to be modelled correctly, installed capacities were set at  
 382 1.4 times the MEC values. This scaling factor was estimated by analysing  
 383 proprietary data from individual solar PV farms provided by EirGrid, which  
 384 showed that, on average, assuming that the installed capacities of farms ex-  
 385 ceed their MEC values by 40% yields the best agreement with the observed  
 386 availability.

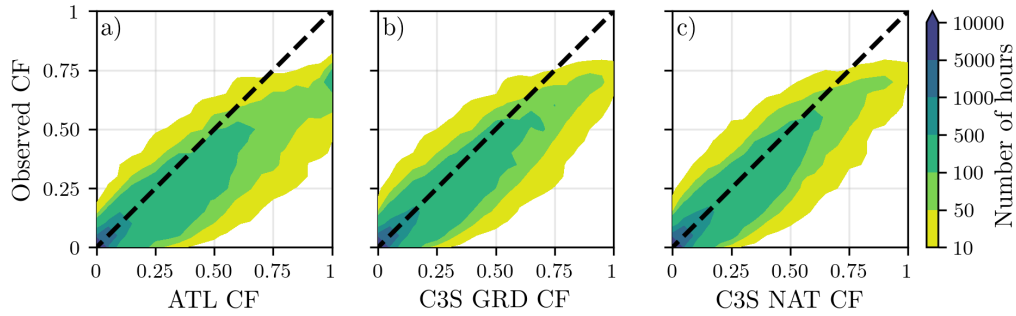


Figure 6: Solar PV CF density plot of the observed (vertical axes) and modelled (horizontal axes) CF series for the a) AtliteATL, b) C3S-E-GC3S GRD and c) C3S-E-NmodelsC3S NAT datasets

387 FigureFig. 6 shows that the three datasets have a similar tendency to  
 388 overestimate the CF compared to the observed values, especially for high CF  
 389 values. The skill scores presented in Table 3 indicate that C3S-E-Gperforms  
 390 best overall, with the lowest RMSE and a high correlation coefficient, suggesting  
 391 a closer match to observed data. All models show a slight positive bias, with  
 392 Atlite exhibiting a slightly lower correlation and higher RMSEC3S GRD and  
 393 C3S NAT perform better than ATL for solar PV CF, with lower RMSE and  
 394 MBE, and higher CC scores. This may be due to the statistical approach  
 395 taken by C3SE for the orientation of the PV panels.

396 Fig. 7 shows the number of solar PV drought events during the 2023  
 397 validation period across different duration ranges. The figure reveals partial  
 398 agreement between the three datasets and the observed data, with consistent  
 399 results noticed for duration ranges of 1-2, 3-4, 7-8, and 8+ days. However,  
 400 discrepancies appear in the other ranges, where the modelsdatasets diverge

	<del>Atlite</del> ATL	<del>C3S-E-G</del> C3S GRD	<del>C3S-E-N</del> C3S NAT
CC	0.921	0.931	0.931
RMSE	0.119	0.090	0.113
MBE	0.046	0.027	0.021

Table 3: Skill scores for solar PV CF for the three datasets compared to observed data

401 from the observed data. The main challenge in validating solar PV data stems  
402 from the recent installation of a large share of Ireland’s solar PV capacity,  
403 with over 65% of the total solar PV capacity installed in 2023. This results in  
404 uncertainties in solar PV generation data and the actual generating capacity  
405 in the first few months after each farm is connected.

406 ~~As the goal of this analysis is to assess the combination of wind and~~  
407 ~~PV generation, the complementary nature of these energy sources mitigates~~  
408 ~~the limitations in PV-only results~~Overall, C3S GRD performs slightly better  
409 than the other datasets in reproducing observed solar PV drought events.

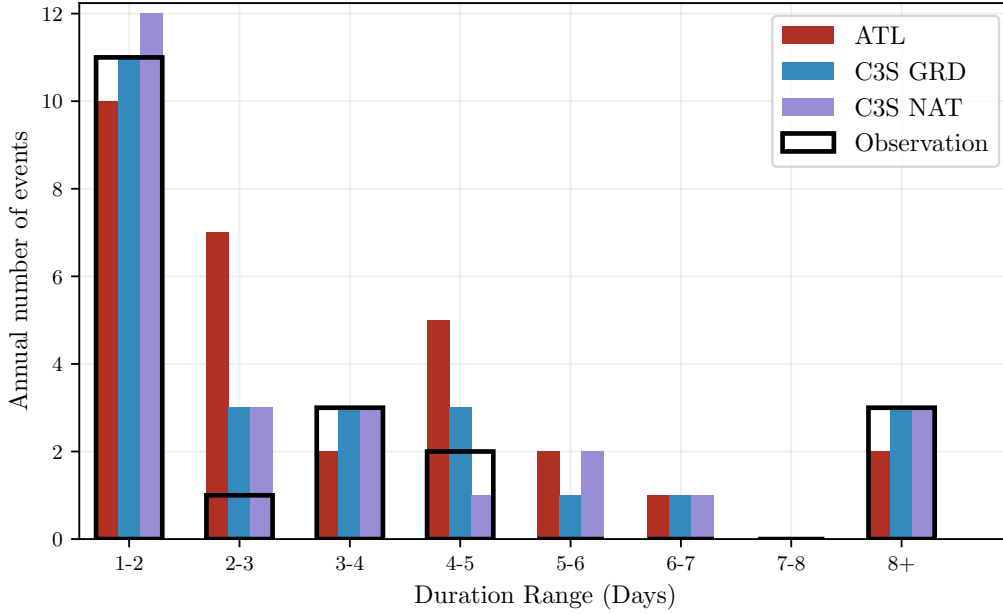


Figure 7: Number of solar PV drought events for ~~Atlite~~ATL (red), ~~C3S-E-G~~C3S GRD (blue), and ~~C3S-E-N~~C3S NAT (purple) and the observed data (black outline). The solar PV droughts are identified for 2023, considering the actual capacity of the system at any given time

## 4.2. Analysis

In this section, RES droughts are analysed by calculating the frequency and duration of RES drought events, the return periods for different RES drought durations, and the seasonality of RES drought events. Understanding the characteristics and timing of RES drought events enables system operators to optimally plan for reserve capacity requirements, ensuring grid stability and security of supply. Results are presented for the three datasets, allowing their differences on the characterisation of RES droughts to be clearly identified.

RES drought events are evaluated under two different scenarios with fixed installed capacities: the 91W-9PV scenario, with 5.9 GW of wind capacity and 0.6 GW of solar PV capacity; and the 57W-43PV scenario, where wind capacity comprises 11.45 GW and solar PV capacity increases to 8.6 GW. Both scenarios were driven by 45 years of ERA5 data. Using the RES drought identification process described in Section 3.5, wind and solar PV droughts are first analysed separately before presenting the results for combined (wind + solar PV) RES droughts under both scenarios.

### 4.2.1. Annual Number of RES Droughts

The first part of the analysis examines the annual number of RES drought events across the three datasets. When only wind energy is considered (Fig. 8a), the number of RES drought events decreases as the duration range increases, with very few events lasting more than seven days. In the case of only contrast, for solar PV energy (Fig. 8b), the number of events also declines as the duration range extends. RES drought frequency declines from one to eight days, followed by a slight increase and then slightly increases for longer durations. This increase occurs because Ireland, being located above the 50° parallel, experiences reduced sunlight during the winter months. From behaviour is attributable to Ireland's high-latitude location, where reduced sunlight in winter (from November to March, PV output often remains consistently low, leading to extended periods where generation stays below the CF threshold) leads to consistently low solar PV output.

When comparing wind and PV results (Fig. 8a & b), Moreover, the comparison between wind and solar PV results indicates that the median, first, and third quartiles for solar PV are consistently higher than or equal to those for wind, across all duration ranges and datasets. This is due to the typically lower CF of PV power compared to wind power, especially in a region such as Ireland where solar potential is limited. expected, given that

447 solar PV generation is ~~also inherently lower,~~ zero at night ~~and constrained~~  
448 ~~by the daily solar cycle, leading to a naturally higher frequency of drought~~  
449 ~~events in PV compared to wind.~~

450 Fig. 8c & d show the combination of wind and PV under the two capacity  
451 ~~scenarios. In the , and limited by the solar cycle.~~ When wind and solar  
452 ~~PV are combined under the 91W-9PV scenario (Fig. 8c), the identified~~  
453 ~~RES droughts closely match those for results closely mirror those of wind~~  
454 ~~alone, which is expected due to the dominance of installed wind capacity.~~  
455 ~~In contrast, wind power in the current energy mix. However, in the 57W-~~  
456 ~~43PV scenario (Fig. 8d) shows a clear reduction in the number of drought~~  
457 ~~events, a marked reduction in RES drought events is observed across all~~  
458 ~~datasets and durations, with a decrease of the total number of events of~~  
459 ~~56% for Atlite ATL, 52% for C3S-E-C3S GRD, and 50% for C3S-E-N.~~  
460 ~~This reduction is attributed to the anti-correlation between wind and PV~~  
461 ~~generation C3S NAT, demonstrating the beneficial effects of a more equal~~  
462 ~~share of wind and solar PV capacity.~~

463 The median, first, and third quartiles for the Atlite dataset are consistently  
464 ~~greater than or equal to those of the other two datasets, regardless of the~~  
465 ~~duration range or type of renewable energy considered. This difference~~  
466 ~~arises from the consistently higher RES drought counts reported by the ATL~~  
467 ~~dataset, compared to the C3S datasets, underscore the importance of wind~~  
468 ~~turbine power curve model used in the C3S-E datasets, which tends to~~  
469 ~~overestimate the wind CF (Fig. 4). As a result, the overall number of RES~~  
470 ~~droughts is underestimated in the C3S-E datasets compared to Atlite representation~~  
471 ~~when quantifying RES droughts. Whereas the three datasets agree on the~~  
472 ~~overall effect of balancing the share of wind and solar PV generation, they~~  
473 ~~differ at a quantitative level, which has crucial implications for energy planning.~~

#### 474 4.2.2. Return Periods of RES Drought Duration

475 ~~The~~ RES drought events identified over the 45-year period were used to  
476 calculate the return periods for different RES drought durations. A return  
477 period is the estimated average time interval between events of a specified  
478 duration ~~or intensity~~ (not to be confused with the frequency of their oc-  
479 currence within a fixed time frame). Fig. 9 ~~illustrates shows~~ the return  
480 periods for ~~varying different~~ RES drought durations, ~~highlighting how often~~  
481 ~~different drought lengths are likely to occur across the datasets. This analysis~~  
482 ~~provides insight into the frequency and likelihood of prolonged low-generation~~  
483 ~~periods, which is crucial for evaluating the potential impact of RES droughts~~

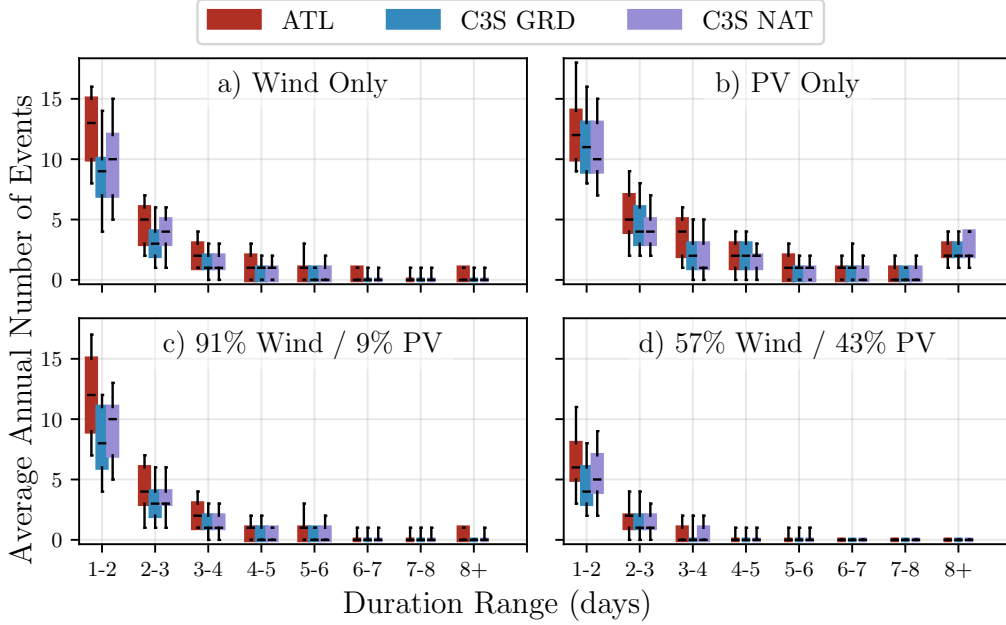


Figure 8: Average annual number of RES droughts (from 1979 to 2023) for a) Wind, b) solar PV, c) 91W-9PV and d) 57W-43PV for Atlite-ATL (red), C3S-E-G-C3S GRD (blue), and C3S-E-N-C3S NAT (purple). The x-axis represents duration ranges in days (lower bound included), while the y-axis indicates the annual number of events. The boxes display the first and third quartiles and the median is marked by a black line. The whiskers indicate the 5th and 95th percentiles

484 ~~on energy reliability and which can be used to capture the most extreme~~  
 485 ~~events affecting the system. Understanding their return periods is crucial, as~~  
 486 ~~extreme yet rare RES droughts pose the toughest challenge to energy security~~  
 487 ~~by placing significant strain on the conventional backup sources necessary to~~  
 488 ~~maintain~~ security of supply ~~during these events.~~

489 The duration of wind droughts (Fig. 9a) increases in a log-linear fashion  
 490 across the three datasets. The log-linear trend indicates a predictable rela-  
 491 tionship between wind drought duration and occurrence, with longer wind  
 492 droughts becoming exponentially less likely as duration increases.

493 In the case of solar PV droughts (Fig. 9b), Atlite behaves differently than  
 494 the two C3S-E-C3S datasets. The Atlite-results-ATL dataset show a generally  
 495 log-linear increase. For C3S-E-G-and-C3S-E-N-C3S GRD and C3S NAT, the  
 496 duration of PV droughts increases in a log-linear pattern for events lasting

less than 16 days. Beyond this duration, there is a sharp rise in solar PV drought duration for events up to a one-year return period. This sudden increase again reflects the impact of extended periods of low PV generation during winter in Ireland.

The difference between ~~Atlite and the C3S-E~~ the ATL and the C3S results arises from differences in the datasets near the threshold of 0.1 CF. ~~Atlite~~ ATL remains slightly above the threshold more frequently during these conditions, leading to shorter, more fragmented RES drought events. In contrast, ~~C3S-E-G and C3S-E-N~~ C3S GRD and C3S NAT tend to fall below the threshold in similar conditions, resulting in longer continuous RES drought periods, especially during winter.

~~For Under~~ the 91W-9PV scenario (Fig. 9c), the combined RES drought return periods mirror those ~~of Fig. 9a, due to the low levels of installed PV capacity. In for wind alone, reflecting the dominance of wind in the current energy mix. In contrast,~~ the 57W-43PV scenario (Fig. 9d) ~~, the return periods for RES droughts increase across all durations~~ shows a dramatic reduction in RES drought durations, suggesting that a more balanced share of wind and solar PV capacity can substantially mitigate the frequency of prolonged RES drought events. For example, the return period for a five-day RES drought event (shown by the vertical dashed lines in Fig. 9) ~~extends-increases~~ from roughly six months for the 91W-9PV scenario, to four years for the 57W-43PV scenario in the ~~Atlite-ATL~~ dataset, and from about fifteen months to around five years in the two ~~C3S-E~~ C3S datasets. This result indicates that the complementarity between wind and solar PV plays a crucial role in reducing the occurrence of RES drought events in a diversified energy portfolio.

Across Fig. 9a, c, and ~~,d~~, the return periods in the ~~Atlite-ATL~~ dataset are consistently higher than those in the two ~~C3S-E~~ C3S datasets. For instance, in the 91W-9PV scenario (Fig. 9c), an event with a one-year return period lasts six days in the ~~Atlite-ATL~~ dataset, compared to only five days in the ~~C3S-E~~ C3S datasets. This difference underscores the importance of ~~model~~ dataset selection when quantifying RES droughts, as each ~~model~~ dataset's assumptions and parametrisations significantly influence ~~drought~~ RES droughts duration estimates. Additionally, in all four graphs, the similarity between results from the two ~~C3S-E~~ C3S datasets suggests that assumptions in the ~~Atlite model-ATL dataset~~, such as wind turbine power curve selection and PV panel specifications—, have a greater impact on RES drought duration estimates than the precise geographic distribution of RES farms when study-

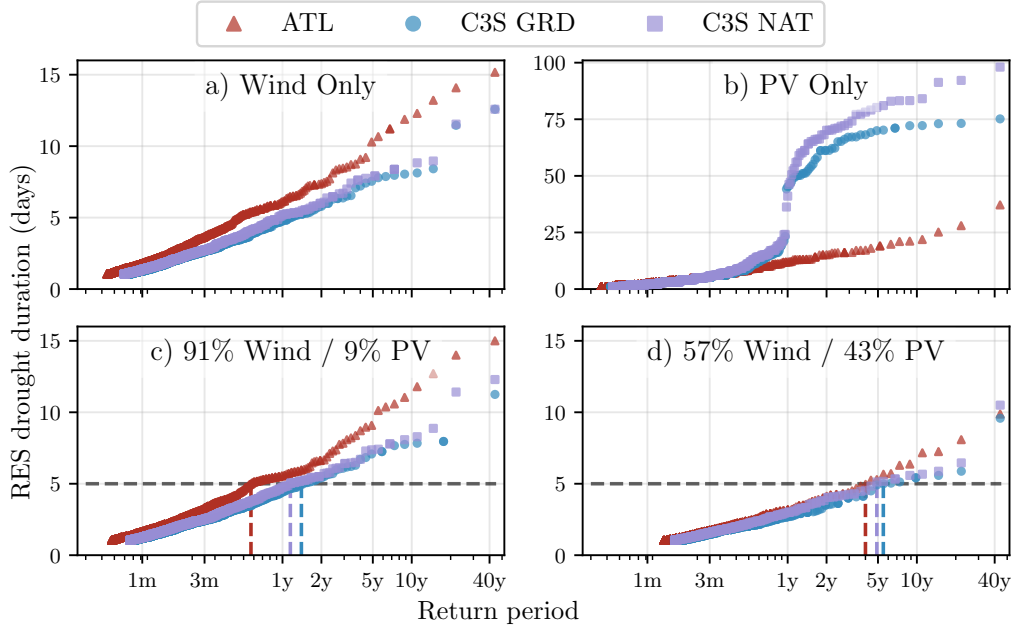


Figure 9: Return periods of the duration of RES droughts (from 1979 to 2023) for a) Wind, b) Solar PV, c) 91W-9PV and d) 57W-43PV for Atlite-ATL (red triangle), C3S-E-G C3S GRD (blue circle), and C3S-E-N C3S NAT (purple square). The x-axis represents the return period time in a log-scale and the y-axis indicates the duration of RES drought associated with it. The horizontal dashed line marks the 5-day return period, with coloured vertical dashed marking its return period for each dataset

ing the return periods of RES droughts.

The return periods calculated from the three datasets show large differences, in particular for the more extreme events with longer return periods. The C3S datasets produce shorter RES drought durations for these events, which would have the largest impact on the power system. This shows that system planning based on the wrong datasets could yield an underestimation of the duration of extreme RES droughts, potentially leading to shortages linked to undersized reserve capacity.

#### 4.2.3. Seasonal Distribution of RES Droughts

The ~~seasonality~~ seasonal analysis of RES droughts ~~was analysed by comparing~~ is based on the percentage of hours in each month classified as part of a RES drought event. Wind droughts tend to be more frequent during summer, whereas solar PV droughts are more common in winter due to reduced

sunlight. By comparing these seasonal patterns across different datasets and energy scenarios, this study examines how dataset-specific assumptions and variations in capacity mix affect the overall characterisation of RES drought events.

For wind-dominated scenarios the wind-only scenario (Fig. 10a & e), the percentage of hours that are part of a drought is higher in summer than in winter. In the Atlite dataset, for instance, an average of ATL dataset exhibits a pronounced seasonal pattern, with about 24% of hours in summer (June-July-August) are identified as wind droughts, summer hours (June, July, August) identified as RES droughts compared to only 4% in winter (December-January-February December, January, February). This seasonal variation is less prominent for the two C3S-E datasets compared to the Atlite one. This difference can be linked to the shape of the two power curves (Fig. 3). CFs near or under strong seasonal signal is less evident in the C3S datasets, which suggests that the differences in the underlying wind power curves play a significant role. In ATL, CF near or below the 0.1 threshold occur at occurs at relatively higher wind speeds for the Atlite power curve than for the C3S-E one, resulting in a higher count of RES drought hours during the summer months. In contrast, the results for solar PV droughts (Fig. 10b) show a higher percentage in winter, with PV droughts occurring display an opposite seasonal trend. Across all datasets, over 60% of the time regardless of the dataset. The Atlite results show a winter hours are classified as solar PV droughts, reflecting the naturally low solar irradiance in Ireland during winter.

ATL tends to record a slightly higher percentage of PV-RES drought hours for wind, and a slightly and a marginally lower percentage for PV, compared to the two C3S-E datasets.

Percentage of hours in a month which are part of a RES drought (from 1979 to 2023) for a) Wind, b) PV, c) 91W-9PV and d) 57W-43PV for Atlite (red dotted), C3S-E G (blue dashed), and C3S-E N (purple solid). The x-axis represents the month of the year, and the y-axis indicates the percentage of hours. Lines correspond to the median values and the area between the first and third quartiles is shaded. Note the different y-axis scale for b). solar PV relative to the C3S datasets. These differences highlight how dataset-specific assumptions, such as the treatment of wind turbine power curves and PV panel characteristics, influences the seasonal dynamics of RES droughts.

The 91W-9PV scenario (Fig. 10c) shows patterns comparable similar to the ones for wind droughts (Fig. 10a). However, in the 91W/9PV scenario,



the number of hours classified as RES droughts in summer decreases slightly compared to the wind-only scenario. This reduction can be explained by the contribution of solar PV generation during the summer months in the 91W-9PV scenario, even though it constitutes only ~~44~~9% of total capacity. Since the number of RES drought hours for solar PV in summer is near zero, this small contribution has a noticeable impact on reducing overall RES drought hours. In the 57W-43PV scenario (Fig. 10d), all three datasets show a reduction in monthly RES drought frequency. Annual reductions in median RES drought frequency are observed across the datasets, dropping from 14% to 5% for ~~Atlite~~ATL, from 8% to 3% for ~~C3S-E-G~~C3S GRD, and from 9% to 4% for ~~C3S-E-N~~C3S NAT. The balanced mix of wind and solar PV power in this scenario reduces the seasonal signal overall and significantly decreases the percentage of RES drought hours in the summer.

## 5. Discussion and Conclusions

~~This study has investigated the ability of three RES models to represent RES droughts : Atlite, C3S-E-G, and C3S-E-N. One of the most evident differences is how each dataset incorporates the specific locations of RES farms. Both Atlite and C3S-E-G consider the locations of wind and PV farms, which one would expect to result in a more accurate representation of RES generation. While this approach slightly improves PV models, our analysis indicates that for wind energy , the Atlite dataset performs better overall, especially in its close alignment with observed data for wind generation estimates. This finding suggests that, although the inclusion of RES farm locations is beneficial, the accuracy of the~~ The seasonal variations of RES droughts observed in this study have important implications for energy planning. Energy demand peaks in winter for Northern European countries, making the seasonality of RES model is more strongly influenced by underlying model assumptions, such as selecting an appropriate wind power curve. droughts critical for the sizing of reserve capacity. Our results show that selecting the wrong dataset could severely underestimate RES droughts during winter months, thereby affecting the reliability of the energy system during critical periods. Additionally, the integration of large shares of solar PV in the system leads to a generalised reduction of RES droughts, yet winter months present a slight increase. The natural limitations of solar PV lead to inevitably higher reserve capacity needs during winter months as reliance on RES increases. These types of insights are essential to develop targeted strategies

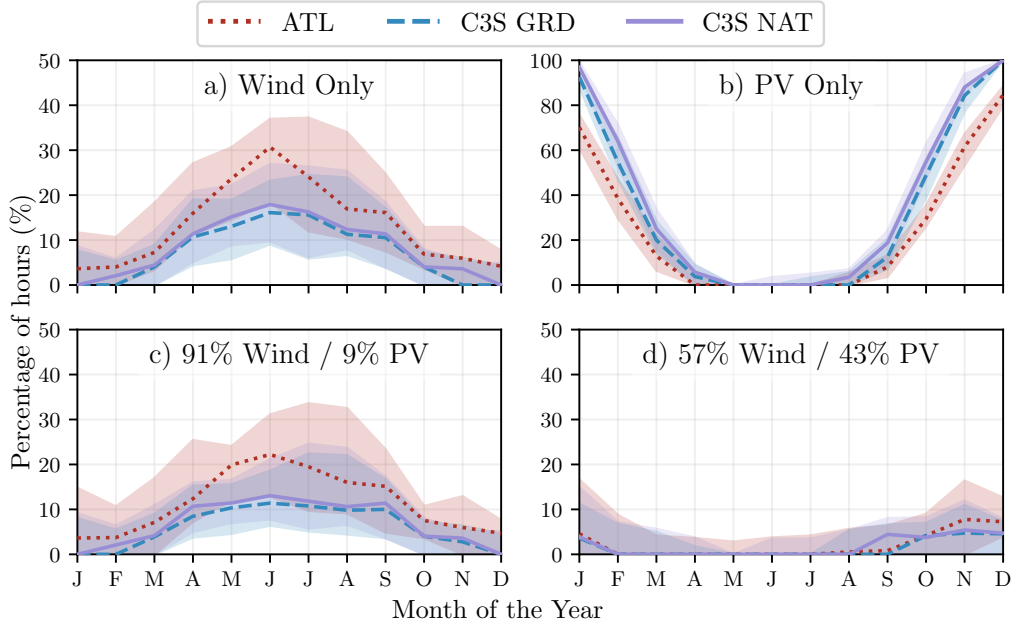


Figure 10: Percentage of hours in a month which are part of a RES drought (from 1979 to 2023) for a) Wind, b) Solar PV, c) 91W-9PV and d) 57W-43PV for ATL (red dotted), C3S GRD (blue dashed), and C3S NAT (purple solid). The x-axis represents the month of the year, and the y-axis indicates the percentage of hours. Lines correspond to the median values and the area between the first and third quartiles is shaded. Note the different y-axis scale for b).

that enhance grid resilience and ensure a stable energy supply throughout the year.

Atlite shows the best alignment with observed data for wind generation. Differences between the models are smaller for PV, with C3S-G performing marginally better than the other two. The results show that the two C3S-E datasets (C3S-E G and C3S-E N) consistently yield similar outcomes, indicating that their methodological differences have minimal impact in this case. This distinction is also evident in the analysis, where Atlite reports higher return periods and a greater number of RES droughts, especially in scenarios with a balanced share of RES. Again, the results from RES drought modelling rely more on the precision of the wind power curve and PV panel model than on the specific locations of RES farms. Atlite's superior performance highlights the importance of selecting validated models for assessing RES drought risks.

~~This careful model selection can better quantify risks, support effective planning  
, and avoid the potential underestimation of capacity needs, which is essential  
for ensuring energy security.~~

## 638 5. Conclusions

639 This study aimed to answer two key questions: Do generic datasets  
640 have sufficient skill to reliably quantify RES drought events? How does the  
641 integration of solar PV into a predominantly wind-based system alter the  
642 characteristics of RES droughts? To address these questions, three datasets  
643 were compared: two derived from the European C3S-Energy dataset, and one  
644 developed by the authors. The datasets derived from C3S-Energy differ in  
645 their assumptions, one assumes a homogeneous distribution of wind and solar  
646 PV capacity across the region, while the other includes the actual locations of  
647 RES farms. The dataset developed by the authors uses a regionally validated  
648 model which accounts for farm locations and uses tailored wind and solar PV  
649 models selected to represent the actual generation.

650 Our results demonstrate that datasets without regional validation misrepresent  
651 the frequency and duration of RES drought events due to their limited  
652 ability to reproduce the observations. The inclusion of wind and solar PV  
653 farm locations has limited impact on RES drought analysis compared to  
654 the choice of wind turbine power curves and solar PV models. Whereas all  
655 three datasets capture broad trends in the duration and seasonality of RES  
656 drought events, the actual number of events is consistently underestimated  
657 by the non-validated datasets. This effect becomes clearer for extreme events,  
658 as not using regionally validated datasets can yield an overestimation of the  
659 return periods of RES droughts. This can lead to insufficient reserve capacity  
660 planning and potential risks to grid stability and security of supply.

661 ~~Looking at the 57W-43PV scenario, the analysis showed a significant  
662 improvement in the management of RES droughts due to the complementary  
663 nature.~~ The effect of the integration of solar PV capacity in a wind-dominated  
664 system on RES droughts has been explored. Our analysis has demonstrated  
665 that transitioning to a system with more equal amounts of wind and PV  
666 generation. Wind and PV together perform better in terms of reducing  
667 drought frequency and duration than either would individually, largely because  
668 of the seasonal anti-correlation between the two energy sources. This diversification  
669 reduces the seasonal impact on RES droughts, as PV generation peaks in the  
670 summer and wind generation is more consistent in winter. Ireland currently

671 has a highly wind-dependent energy system, but with ambitious targets  
 672 for PV installations in the coming years, the energy mix is expected to  
 673 approach a balance between wind and PV capacity. While this balanced  
 674 approach offers a more stable and secure energy supply by mitigating RES  
 675 drought risks, it is important to note that having similar wind and PV  
 676 capacities may not optimise other aspects, such as annual energy production  
 677 or meeting nighttime loads. For policymakers, these findings underscore  
 678 the importance of meeting these capacity targets to enhance energy security  
 679 through diversification. Additionally, the choice of model for RES drought  
 680 assessment becomes increasingly critical as more renewable capacity is integrated  
 681 into the system. solar PV capacity reduces the occurrence of RES drought  
 682 events, mitigates extreme RES drought conditions and enhances overall system  
 683 resilience. This improvement is attributed to the complementary nature of  
 684 wind and solar PV generation, as solar PV generation typically peaks in  
 685 summer while wind generation predominates during winter. However, this  
 686 integration is unable to counter critical winter RES droughts, which coincide  
 687 with the strongest electricity demand in Northern European countries.  
 688 The results presented in this study have three main limitations. First,  
 689 the definition of RES droughts based on generation does not consider the  
 690 important role of demand, which could be of interest to system operators.  
 691 Second, recent solar PV capacity expansions have changed the generation  
 692 profile, limiting solar PV data for model training to a single year, although a  
 693 longer validation period would be preferable. Third, the source for weather  
 694 data is ERA5 has limited spatial resolution, an issue that can be addressed  
 695 once higher resolution datasets become available.  
 696 Future work is planned to extend the current analysis. First, climate pro-  
 697 jection data will be integrated with different energy scenarios, incorporating  
 698 the addition of offshore wind, to better understand how climate change **might**  
 699 and offshore wind may affect RES droughts. Second, expanding the geo-  
 700 graphic domain of the study to include the rest of Europe, while also including  
 701 the role of electricity interconnects between countries, would provide a more  
 702 comprehensive understanding of RES droughts ~~in an interconnected energy~~  
 703 ~~grid~~. This would require extensive verification across other European coun-  
 704 tries, making it a more complex but highly relevant challenge.

## Data Availability

The ERA5 data can be obtained from the Climate Data Store (<https://doi.org/10.24381/cds.adbb2d47>). The ~~C3S-E~~-C3SE dataset is also available from the Climate Data Store (<https://doi.org/10.24381/cds.4bd77450>). Information on wind and solar PV farms in Ireland can be obtained from the EirGrid website (<https://www.eirgrid.ie/grid/system-and-renewable-data-reports>). The Atlite model used in this study is open-source and can be found on GitHub (<https://github.com/pypsa/atlite>). The data and code required to reproduce the analysis in this article will be made available upon acceptance of the manuscript in a public GitHub repository.

## Acknowledgments

The research conducted in this publication was funded by Science Foundation Ireland and co-funding partners under grant number 21/SPP/3756 through the NexSys Strategic Partnership Programme.

## References

- [1] EuroStat, Renewable Energy Statistics, 2023. URL: [https://ec.europa.eu/eurostat/statistics-explained/index.php?title=Renewable\\_energy\\_statistics](https://ec.europa.eu/eurostat/statistics-explained/index.php?title=Renewable_energy_statistics), Accessed: 2024-11-06.
- [2] H. C. Bloomfield, D. J. Brayshaw, L. C. Shaffrey, P. J. Coker, H. E. Thornton, Quantifying the increasing sensitivity of power systems to climate variability, *Environmental Research Letters* 11 (2016) 124025. doi:10.1088/1748-9326/11/12/124025.
- [3] H. C. Bloomfield, D. J. Brayshaw, A. Troccoli, C. M. Goodess, M. De Felice, L. Dubus, P. E. Bett, Y.-M. Saint-Drenan, Quantifying the sensitivity of european power systems to energy scenarios and climate change projections, *Renewable Energy* 164 (2021) 1062–1075. doi:10.1016/j.renene.2020.09.125.
- [4] K. van der Wiel, L. P. Stoop, B. R. H. Van Zuijlen, R. Blackport, M. A. Van den Broek, F. M. Selten, Meteorological conditions leading to extreme low variable renewable energy production and extreme high energy shortfall, *Renewable and Sustainable Energy Reviews* 111 (2019) 261–275. doi:10.1016/j.rser.2019.04.065.

- 738 [5] F. Kaspar, M. Borsche, U. Pfeifroth, J. Trentmann, J. Drücke, P. Becker,  
739 A climatological assessment of balancing effects and shortfall risks of  
740 photovoltaics and wind energy in germany and europe, *Advances in*  
741 *Science and Research* 16 (2019) 119–128. doi:10.5194/asr-16-119-2  
742 019.
- 743 [6] M. Ohba, Y. Kanno, D. Nohara, *Climatology of dark doldrums in japan,*  
744 *Renewable and Sustainable Energy Reviews* 155 (2022) 111927. doi:10  
745 .1016/j.rser.2021.111927.
- 746 [7] F. Mockert, C. M. Grams, T. Brown, F. Neumann, *Meteorological*  
747 *conditions during periods of low wind speed and insolation in Germany:*  
748 *The role of weather regimes,* *Meteorological Applications* 30 (2023)  
749 e2141. doi:10.1002/met.2141.
- 750 [8] M. J. Mayer, B. Biró, B. Szücs, A. Aszódi, *Probabilistic modeling of*  
751 *future electricity systems with high renewable energy penetration using*  
752 *machine learning,* *Applied Energy* 336 (2023) 120801. doi:10.1016/j.  
753 apenergy.2023.120801.
- 754 [9] D. Raynaud, B. Hingray, B. François, J. Creutin, *Energy droughts from*  
755 *variable renewable energy sources in European climates,* *Renewable*  
756 *Energy* 125 (2018) 578–589. doi:https://doi.org/10.1016/j.renene  
757 .2018.02.130.
- 758 [10] K. Z. Rinaldi, J. A. Dowling, T. H. Ruggles, K. Caldeira, N. S. Lewis,  
759 *Wind and Solar Resource Droughts in California Highlight the Benefits*  
760 *of Long-Term Storage and Integration with the Western Interconnect,*  
761 *Environmental Science and Technology* 55 (2021) 6214–6226. doi:10.1  
762 021/acs.est.0c07848.
- 763 [11] A. Gangopadhyay, A. K. Seshadri, N. J. Sparks, R. Toumi, *The role*  
764 *of wind-solar hybrid plants in mitigating renewable energy-droughts,*  
765 *Renewable Energy* 194 (2022) 926–937. doi:10.1016/j.renene.2022.  
766 05.122.
- 767 [12] S. Allen, N. Otero, *Standardised indices to monitor energy droughts,*  
768 *Renewable Energy* 217 (2023) 119206. doi:10.1016/j.renene.2023.11  
769 9206.

- 770 [13] J. Kapica, J. Jurasz, F. A. Canales, H. Bloomfield, M. Guezgouz,  
771 M. De Felice, Z. Kobus, The potential impact of climate change on  
772 european renewable energy droughts, *Renewable and Sustainable En-  
773 ergy Reviews* 189 (2024) 114011. doi:10.1016/j.rser.2023.114011.
- 774 [14] P. T. Brown, D. J. Farnham, K. Caldeira, Meteorology and climatology  
775 of historical weekly wind and solar power resource droughts over western  
776 North America in ERA5, *SN Applied Sciences* 3 (2021) 814. doi:10.1  
777 007/s42452-021-04794-z.
- 778 [15] C. Bracken, N. Voisin, C. D. Burleyson, A. M. Campbell, Z. J. Hou,  
779 D. Broman, Standardized benchmark of historical compound wind and  
780 solar energy droughts across the Continental United States, *Renewable  
781 Energy* 220 (2024) 119550. doi:https://doi.org/10.1016/j.renene  
782 .2023.119550.
- 783 [16] H. Lei, P. Liu, Q. Cheng, H. Xu, W. Liu, Y. Zheng, X. Chen, Y. Zhou,  
784 Frequency, duration, severity of energy drought and its propagation in  
785 hydro-wind-photovoltaic complementary systems, *Renewable Energy*  
786 (2024) 120845. doi:10.1016/j.renene.2024.120845, 2.
- 787 [17] H. Hersbach, B. Bell, P. Berrisford, S. Hirahara, A. Horányi, J. Muñoz-  
788 Sabater, J. Nicolas, C. Peubey, R. Radu, D. Schepers, et al., The ERA5  
789 global reanalysis, *Quarterly Journal of the Royal Meteorological Society*  
790 146 (2020) 1999–2049. doi:10.1002/qj.3803.
- 791 [18] L. Dubus, Y. Saint-Drenan, A. Troccoli, M. De Felice, Y. Moreau, L. Ho-  
792 Tran, C. Goodess, R. Amaro E Silva, L. Sanger, C3S Energy: A climate  
793 service for the provision of power supply and demand indicators for Eu-  
794 rope based on the ERA5 reanalysis and ENTSO-E data, *Meteorological  
795 Applications* 30 (2023) e2145. doi:10.1002/met.2145.
- 796 [19] Copernicus Climate Change Service (C3S), Climate and energy indi-  
797 cators for Europe from 1979 to present derived from reanalysis., 2020.  
798 doi:10.24381/cds.4bd77450, accessed on 28-11-2024.
- 799 [20] F. Hofmann, J. Hampp, F. Neumann, T. Brown, J. Hörsch, Atlite: a  
800 lightweight Python package for calculating renewable power potentials  
801 and time series, *Journal of Open Source Software* 6 (2021) 3294. doi:10  
802 .21105/joss.03294.

- [21] J. Li, Z. Zhao, D. Xu, P. Li, Y. Liu, M. A. Mahmud, D. Chen, The potential assessment of pump hydro energy storage to reduce renewable curtailment and CO2 emissions in Northwest China, *Renewable Energy* 212 (2023) 82–96. doi:10.1016/j.renene.2023.04.132.
- [22] M. Parzen, H. Abdel-Khalek, E. Fedotova, M. Mahmood, M. M. Fryszacki, J. Hampp, L. Franken, L. Schumm, F. Neumann, D. Poli, et al., Pypsa-earth. a new global open energy system optimization model demonstrated in africa, *Applied Energy* 341 (2023) 121096. doi:10.1016/j.apenergy.2023.121096.
- [23] K. Ali Khan Niazi, M. Victoria, Comparative analysis of photovoltaic configurations for agrivoltaic systems in europe, *Progress in Photovoltaics: Research and Applications* 31 (2023) 1101–1113. doi:10.1002/pip.3727.
- [24] A. Kies, B. U. Schyska, M. Bilousova, O. El Sayed, J. Jurasz, H. Stoecker, Critical review of renewable generation datasets and their implications for european power system models, *Renewable and Sustainable Energy Reviews* 152 (2021) 111614. doi:10.1016/j.rser.2021.111614.
- [25] EirGrid & SONI, System and Renewable Data Reports, 2023. URL: <https://www.eirgrid.ie/grid/system-and-renewable-data-reports>, Accessed: 2024-11-06.
- [26] N. Otero, O. Martius, S. Allen, H. Bloomfield, B. Schaeffli, Characterizing renewable energy compound events across Europe using a logistic regression-based approach, *Meteorological Applications* 29 (2022) e2089. doi:10.1002/met.2089, 13.
- [27] Y.-M. Saint-Drenan, L. Wald, T. Ranchin, L. Dubus, A. Troccoli, An approach for the estimation of the aggregated photovoltaic power generated in several European countries from meteorological data, *Advances in Science and Research* 15 (2018) 51–62. doi:10.5194/asr-15-51-2018.
- [28] I. Staffell, S. Pfenninger, Using bias-corrected reanalysis to simulate current and future wind power output, *Energy* 114 (2016) 1224–1239. doi:10.1016/j.energy.2016.08.068.



- 836 [29] Government of Ireland, Climate Action Plan 2024, Technical Report 3,  
837 Department of the Environment, Climate and Communications, 2023.  
838 URL: [https://www.gov.ie/pdf/?file=https://assets.gov.ie/](https://www.gov.ie/pdf/?file=https://assets.gov.ie/284675/70922dc5-1480-4c2e-830e-295afd0b5356.pdf)  
839 [284675/70922dc5-1480-4c2e-830e-295afd0b5356.pdf](https://www.gov.ie/pdf/?file=https://assets.gov.ie/284675/70922dc5-1480-4c2e-830e-295afd0b5356.pdf), Accessed:  
840 2024-11-06.
- 841 [30] Sustainable Energy Authority Ireland, National Energy Projections  
842 2024, Technical Report, Sustainability Energy Authority of Ireland,  
843 2024. URL: [https://www.seai.ie/news-and-events/news/energ](https://www.seai.ie/news-and-events/news/energy-projections-report)  
844 [y-projections-report](https://www.seai.ie/news-and-events/news/energy-projections-report), Accessed: 2024-11-06.
- 845 [31] EirGrid & SONI, Tomorrow's Energy Scenarios 2023, Technical Report,  
846 EirGrid & SONI, 2023. URL: [https://cms.eirgrid.ie/sites/def](https://cms.eirgrid.ie/sites/default/files/publications/TES-2023-Final-Full-Report.pdf)  
847 [ault/files/publications/TES-2023-Final-Full-Report.pdf](https://cms.eirgrid.ie/sites/default/files/publications/TES-2023-Final-Full-Report.pdf),  
848 Accessed: 2024-11-06.
- 849 [32] H. G. Beyer, G. Heilscher, S. Bofinger, A robust model for the mpp  
850 performance of different types of pv-modules applied for the performance  
851 check of grid connected systems, Eurosun (2004) 8.